2 Part 1: Pilot Plant Trials

2.1.1 Background

Studies into the decrepitation behaviour of TiO_2 slags showed the phenomenon to occur due to oxidation of the M_3O_5 phase to M_6O_{11}.[5,6,7] The accompanying volume change of the crystal appears to initiate the physical breakdown of the material to particles smaller than 100 µm. This reaction was found to occur readily at temperatures between 200 and 600 ºC. (Above 600 ºC oxidation of the M_3O_5 phase results in anatase; at temperatures below 200 ºC, the reaction kinetics was considered to be too slow for the M_3O_5 to M_6O_{11} reaction to proceed.)

As a continuation of this work the objectives of the slag block cooling trials conducted during the 9th 3MVA ilmenite smelting campaign were:

- To quantify the impact of different cooling methods on block decrepitation;
- To investigate the possible impact of the cooling method on the crushing and milling behaviour of those blocks which remained fully or partially intact during cooling.

Slag taps were made from the 3MVA pilot furnace into slag pots with a 1.5 tons TiO_2 slag capacity. The shape of these cast steel bowls resembled that of the 20 t slag bowls intended for the industrial scale plant (Figure 4).

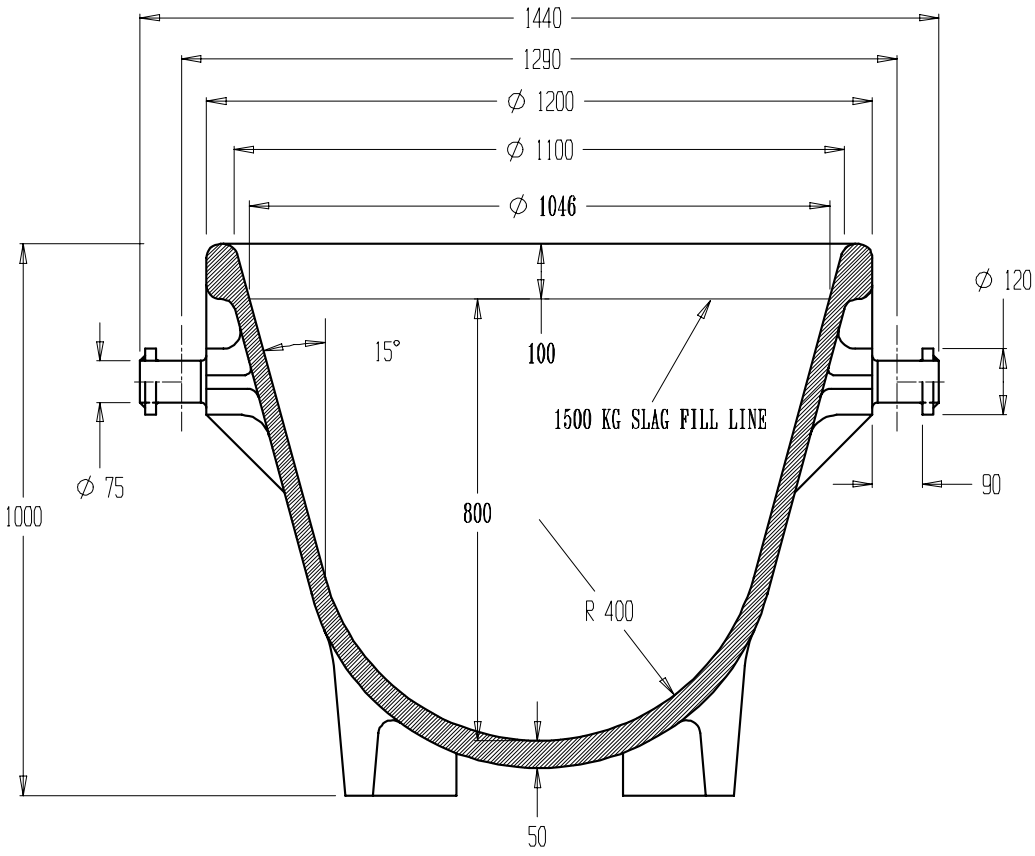

Figure 4 Slag pot with 1.5 t capacity used during the Campaign 9 slag block cooling trials.

2.2 Slag block cooling

2.2.1 Experimental procedure

Following tapping, the slag blocks were left to cool in the pots for 6 to 8 hours. After this period of primary cooling the blocks were tipped out of the pots and cooled under various cooling conditions:

- Air cooling. Apart from one block, each of the blocks cooled in air was tipped onto a 1.2 x 1.2 m steel grid positioned above an steel tray (Figure 5). Any material losses from the block (e.g. due to decrepitation) fell through the grid into the tray enabling the measurement of mass loss over time. One air cooled block was placed on a solid concrete base. All decrepitated material was left to accumulate on and around this block. All the air cooled blocks were left to cool undisturbed, under conditions of natural air cooling.

- Water cooling. These blocks were tipped from the pots onto the grid and tray stands. To enable continuous water cooling over the full block surface, a pipe cage with water sprays was positioned over each block (Figure 6). Apart from the short intervals when surface temperatures of the blocks were measured, these blocks were cooled continuously under water. Surface temperatures were measured using an optical pyrometer with an emissivity setting of 0.8 (during those short periods when the water sprays were turned off).

- Intermittent water cooling. These blocks were tipped onto the grid and tray stands and covered with a water spray cage. As in the case of the water cooled blocks, the water supply was closed when surface temperatures were measured. When such surface temperatures were below 200 ºC, the water supply remained closed. In instances were the surface temperature was above 200 ˚C during follow-up measurements, the water supply was immediately opened. The surface temperatures of these blocks were measured with a handheld pyrometer with an emissivity setting of 0.8. The surface temperatures of one of these blocks during the water-off periods were recorded with a thermographic camera.

- Submerged cooling. Several blocks were submerged directly after tipping into a water tank, through which water was circulated continuously. The period of submersion varied from 1 to 16 hours, with one block being repeatedly submerged. After such a block had been taken out of the water it was placed on a grid and tray stand. Surface temperatures were subsequently measured at hourly intervals, while mass losses (where they occurred) were recorded simultaneously.

- Two blocks were left to cool in the pots. Thermocouples were inserted into one of these blocks directly after tapping. This experiment was repeated during Campaign 10 and is discussed further in Part 3 of this document. For the purposes of Part 1, this block – of which the open end was exposed to air – is compared to the second pot-cooled block which was covered with a lid for the full duration of cooling.

Within these cooling method groupings, block composition (%FeO) and tap mass were varied. A summary of the different blocks, their most important attributes and cooling methods is given in Table 1.

Subsequent to complete cooling, the block yield was calculated for each block by dividing the final remaining block mass by its original tapped mass. Higher block yields indicate less material losses due to decrepitation, and hence a more successful cooling method.

Table 1 Summary of the cooling methods used during the pilot plant trials of Campaign 9.

Cooling method		%FeO	%TiO_2	Block mass (kg)	Block yield (%)	Tap number
Air cooling		7.83	90.18	1,021	37.5	38
		10.39	87.49	1,281	33.6	51
		11.46	85.99	1,420	42.3	64
		9.38	88.03	1,097	10.8	59†
Water cooling		9.74	88.29	622	91.3	49
		9.83	88.03	1,091	96.2	50
		9.60	88.52	1,535	95.9	48
		9.78	87.57	1,557	97.9	60
Intermittent water cooling		9.46	88.82	929	92.4	36
		11.99	85.66	1,017	96.2	42‡
		9.49	88.17	1,099	91.0	37
		10.56	87.01	1,471	90.3	61
Submerged cooling	1 hr	10.22	87.66	986	45.2	46
	2 hrs	10.13	87.78	1,029	50.1	52
	3 hrs	11.06	86.53	1,069	74.5	47
	5 hrs	10.99	86.85	1,133	91.7	45
	8 hrs	10.42	87.43	1,062	92.9	43
	16 hrs	10.17	87.09	1,131	96.2	58
	Repeat	10.71	87.27	1,498	95.2	65
Pot cooled	Uncovered block	10.72	87.06	1,275	nd	62
	Covered block	11.47	86.29	855	nd	44

2.2.2 Results

The surface temperatures of the air cooled blocks over time are shown in Figure 7. The average block yield of the air cooled blocks which were placed on grid and tray stands was 38% (Table 1). Since the particle size distribution of decrepitated material is 80% - 90% below 100 µm (refer to Part 2), 50% to 56% of the original mass of these blocks is therefore immediately classed as the lower valued fine slag, even before any further crushing or milling has been applied.

† Block was placed on solid concrete flooring; decrepitated material hence accumulated around and on the block surface.

‡The surface temperatures of this block were recorded with both a handheld pyrometer and thermographic camera.

Figure 5 Grid and tray stand on which slag blocks were placed to cool

Figure 6 Slag block under water cooling during Campaign 9

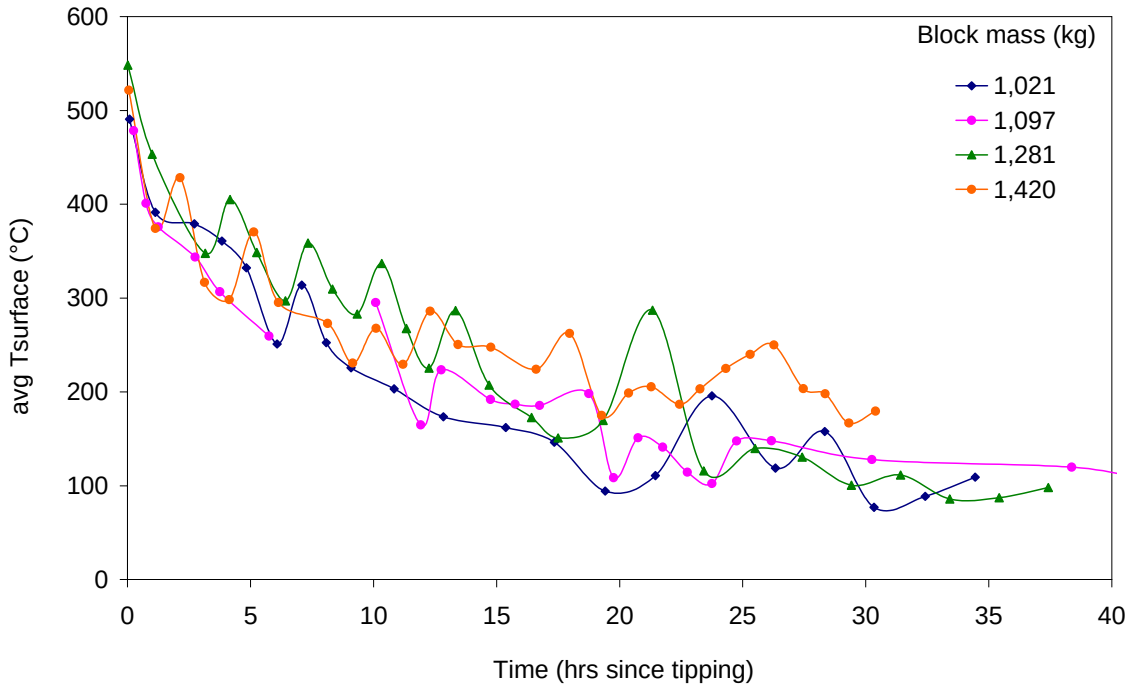

Figure 7 Average surface temperature of slag blocks cooled in air.

In contrast with the other three air cooled blocks, tap 59 was tipped onto a solid concrete floor to cool. Decrepitated material did not fall off and away from the surface of this block through the grid, but accumulated on and around the block surface. Between hours 15 and 50 (counting from the time of tipping), the outer layer (5 – 20 mm) of the decrepitated material was periodically removed at a small localised area and the temperature of the newly exposed surface was measured. These subsurface temperatures, shown as the broken line in Figure 8, were up to 120 ºC higher than the original surface temperatures. An example of the

decrepitated flakes which formed on this block is shown in Figure 9. These flakes were flimsy and broke up into a powder on further handing. The yield of block 59 was 10.8%, and although intact when compared to the decrepitated surface layer, the core was too weak to withstand further handling required for crushing and/or milling.

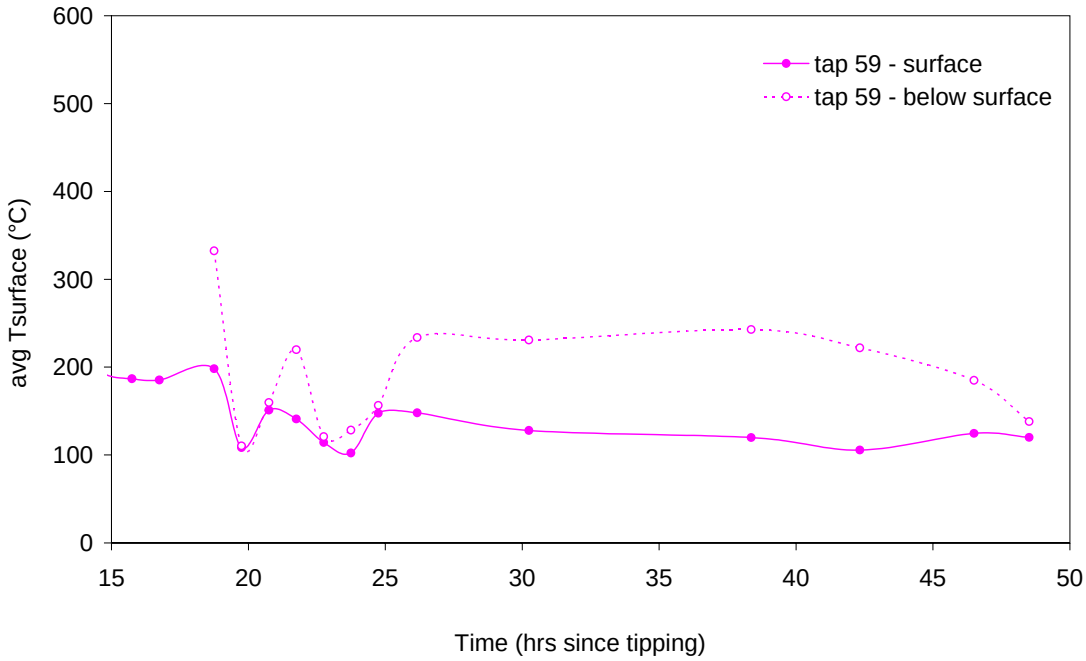

Figure 8 Average surface and subsurface temperatures of tap 59 (isolating block).

Figure 9 Example of decrepitated material showing the flake-like structure which captures air to form an isolating layer round the block when left to accumulate.

The surface temperatures of the water cooled blocks over time are shown in Figure 10. The average yield for these blocks was 93% (Table 1). The surface temperatures of the

intermittently water cooled blocks are shown in Figure 11. The average block yield for these was 95% (Table 1). Clearly the block yields of the water cooled blocks, were markedly higher than those of the air cooled blocks, for both continuous and intermittent water cooling.

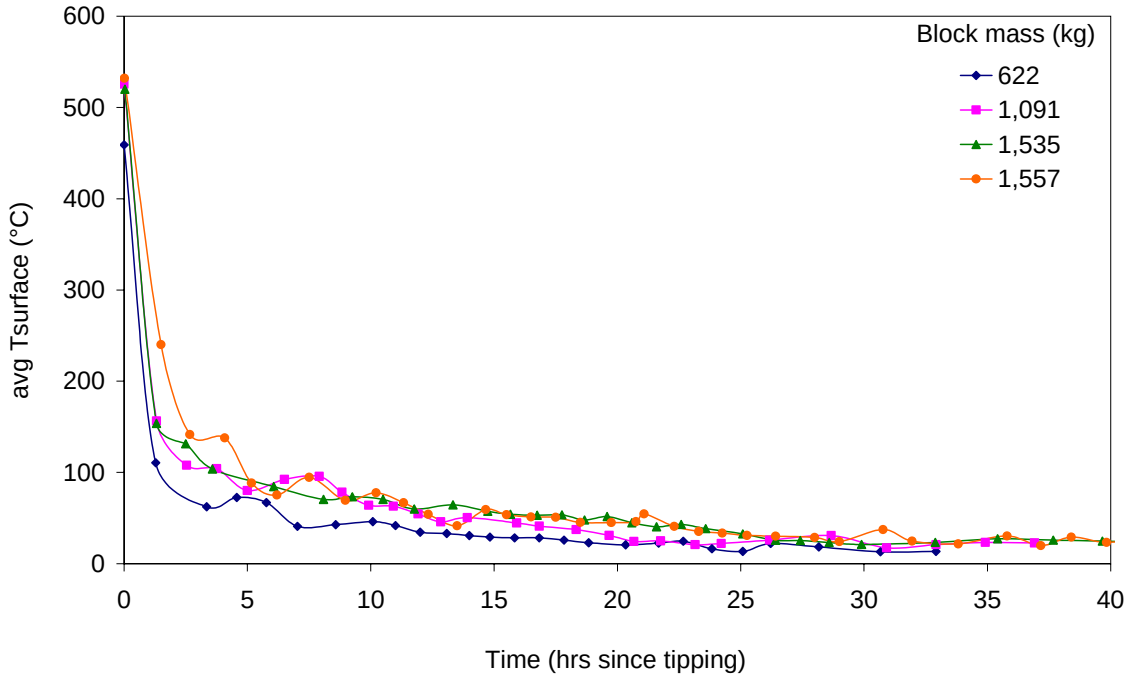

Figure 10 Average surface temperature of blocks cooled continuously with water.

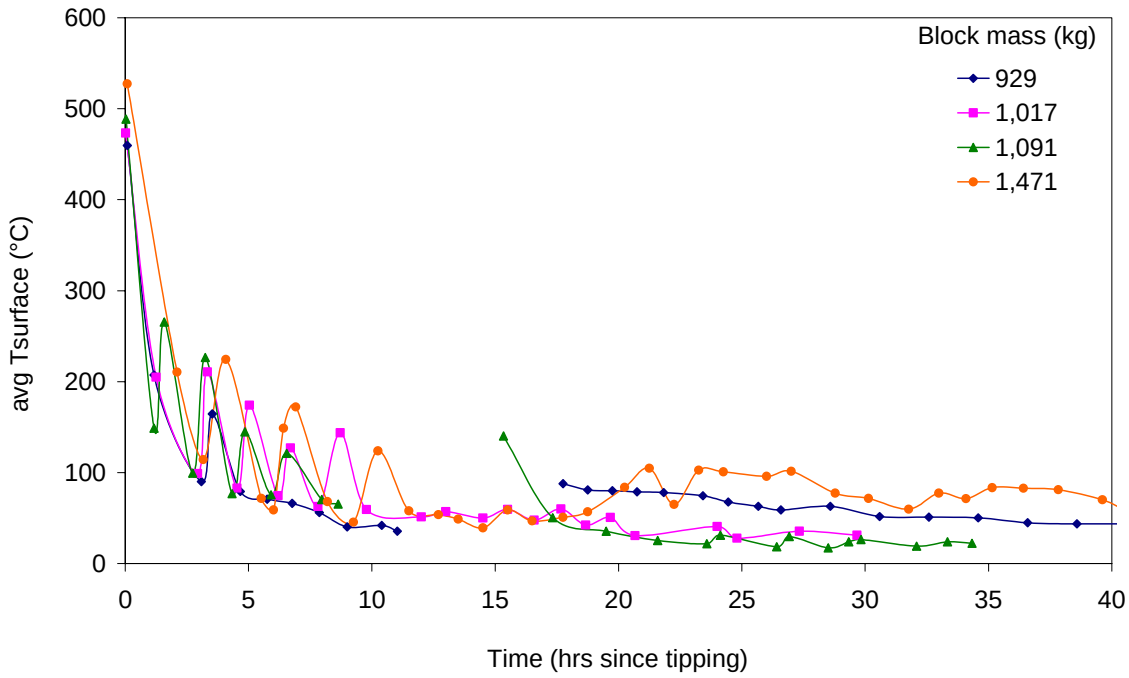

Figure 11 Average surface temperature of blocks cooled intermittently with water.

The measured surface temperatures of the blocks submerged in water are shown in Figure 12. The surface temperatures of these blocks were taken directly after being tipped out of the pots,

and thereafter only when each block was removed from the water tank. One of these blocks was repeatedly submerged until no increase in the surface temperature was detected. This point was reached after 9 submersions, 32.3 hours after closing the taphole. The block yields of the submerged blocks are shown in Table 1. Yields improved significantly with increasing submersion time, with the most significant improvement when the block was cooled for longer than 5 hours before removing it from the water.

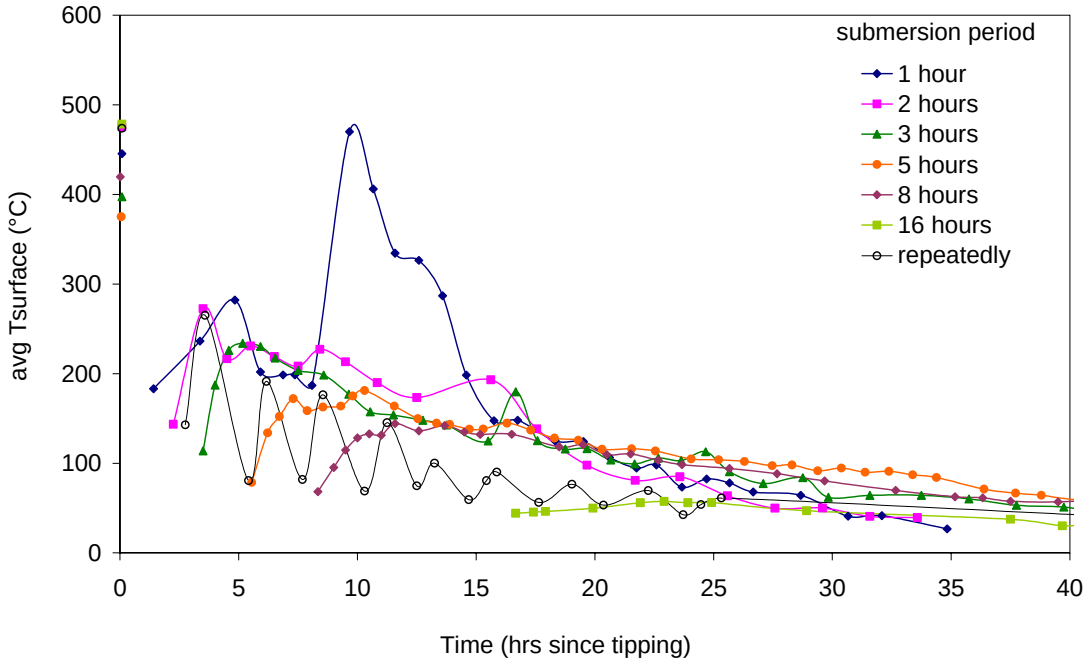

Figure 12 Average surface temperature of blocks after submersion in water.

2.2.3 Conclusions

In terms of block yield, the cooling methods can be classed into four groups:

- Exceptionally poor: natural air cooling combined with accumulation of decrepitated material on and around the block surface.
- Poor: natural air cooling and submerged water cooling for up to 1 hour. These cooling methods resulted in block yields from 33% to 45%.
- Medium: water submersion for 2 to 3 hours. This method resulted in block yields ranging between 50% and 75%.
- Good: continuous and intermittent water cooling to limit the time during which the surface temperature of the block is above 200 ˚C. Water submersion for 5 hours and longer also falls within this group. The block yields from these cooling methods were all above 90%.

The exceptionally poor results recorded where the decrepitated material accumulates is likely due to progressive air ingress between the decrepitation flakes. The combination of slag flakes and air forms an effective thermal insulation layer on the surface of the block. From Figure 8 the temperature within this isolating layer remains in the temperature range where decrepitation is reported to occur[5]. The process therefore becomes self supportive: exposure to air at these

temperatures promotes further decrepitation (by the oxidation reaction) which allows progressively deeper air ingress, which in turn results in decrepitation deeper below the surface. The weakness of the block core is indicative that this process – although not fully complete - progressed into the centre of the block. In the case of the three blocks which were placed on grids, the decrepitated material was removed from the block surface by falling under gravity through the grid. This prevented build-up of a substantial isolating layer, hence allowing a steeper subsurface temperature gradient with less air ingress, effectively limiting decrepitation.

The effect of surface temperature is illustrated by the series of submerged cooled blocks: the yields of blocks which were initially water-cooled by submersion for 3 hours and for 5 hours were 74.5% and 91.7% respectively. The maximum surface temperatures of these blocks were 234 ˚C (3 hours submersion) and 181 ˚C (5 hours submersion). It therefore appears that decrepitation is notably reduced at surface temperatures below around 200 ˚C. Decrepitation furthermore seems to be largely suppressed at surface temperatures lower than 100 ˚C to 80 ˚C: the maximum surface temperature of the block submerged for 8 hours was 144 ˚C, in comparison with 58 ˚C of the block submerged for 16 hours. The corresponding block yields were 92.9% (8 hours submerged) vs. 96.2% (16 hours submerged). This is supported by the surface temperatures of the intermittently water cooled blocks as shown in Figure 11: the highest block yield was from tap 42 with surface temperatures which were consistently below 60 ˚C from 10 hours after tipping and onwards.

The good block yields of the intermittently water cooled blocks despite surface temperatures in the temperature range where decrepitation typically occurs during the initial 10 hours of cooling, is interpreted as an indication of the kinetic component of the decrepitation mechanism; that is, the time spent within the temperature range for decrepitation is also important.

The inclined surfaces of the blocks cooled in the pots showed no indication of any decrepitation: the mould coating§ was still clearly visible on the whole of these surfaces. Varying extents of decrepitation did occur on the horizontal (upper) surfaces of these blocks, however. The block yields of these blocks could unfortunately not be determined accurately since, after standing for a prolonged period in the pot, these blocks were stuck in the pots and broke into several pieces when they were eventually were removed from the pots.

Decrepitation can thus be eliminated or at least be reduced through:

1. removing air from the surface when the surface is at elevated temperatures
2. reducing the surface temperature to below 200 ˚C, but preferably even lower temperatures.
3. limiting the period when the surface is exposed to air when at elevated temperatures.

Block losses of continuously water cooled blocks occurred predominantly as 2 - 10 mm thick crusts peeling from the surface. The appearance of these crusts does not fit in with the

§ A water based slurry containing alumina powder is sprayed on the inside of the pots before every tap to reduce the occurance of blocks sticking to the pot surface.

definition or mechanism of decrepitation. The fact that the block yield for the smallest block (622 kg vs. 1,091 – 1,557 kg) was lowest within the continuously water cooled group (91.3% vs. an average of 96.7%) indicates that the origin of this "peeling" effect is likely to also be surface driven.

No significant correlation between slag composition and block yield was obvious. However, since the chemistry range within the various cooling method groups was narrow (Table 1), this does not rule out the possibility that differences in chemistry might affect block yield. However, for the range tested, if chemistry does play a role, it is overshadowed by the effect of the cooling method.

2.3 Crushing and Milling

2.3.1 Experimental procedure

Out of the blocks discussed in section 2.2 eleven blocks were selected when proceeding with the crushing and milling trials. Details of these blocks are shown in Table 2. A hydraulic press was used to break each individual block down to -200 mm lumps. Each block was individually further crushed down to initially -50 mm particles and then -20 mm particles utilising the Exxaro R&D pilot scale primary and secondary jaw crusher facilities. A 50 kg sample was riffled from the -20 mm product and passed through a roll crusher producing a -2 mm product. The roll diameter of this crusher was 300 mm and had a length of 200 mm. The crusher was driven by a 2.2 kW motor which resulted in a rotating speed of 638 rpm. The roll crusher product was passed over a series of screens following the Canadian Standard Sieve Series[25] between 1400 µm and 75 µm. The +850 µm fraction was circulated back through the roll mill three more times, each time conducting a screen analysis on the product and separating out the +850 µm fraction. This procedure gave four sieve analyses in total for each block.

The breaking and crushing procedure described above (and shown in Figure 13) was accepted at the time as not representative of the material flow or the comminution equipment of the industrial scale slag processing plant (which was still being designed and engineered at the time). Hence, the absolute values of the particle size distributions obtained from these trials were not treated as representative of those experienced on the industrial scale plant. However, since all eleven blocks were broken and crushed according to the same procedure, the value of the test work lies in the comparative conclusions which can be drawn.

Table 2 Blocks produced during campaign 9 which were used for the crushing trials.

Cooling method		Tap number	Block yield (%)
Air cooling		64	42.3
Water & air cooling		36	92.4
		37	91.0
		42	96.2
Water cooling		49	91.3
		60	97.9
Submersion cooling	3 hours	47	74.5
	8 hours	43	92.9
	repeatedly	65	95.2
Pot cooling - covered		44	-
Pot cooling - open		62	-

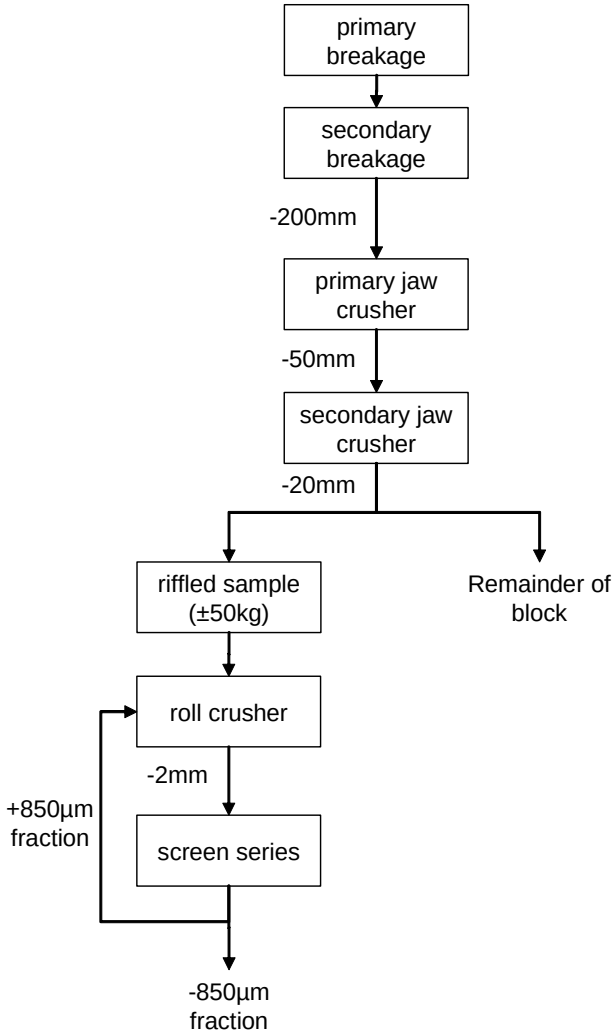

Figure 13 Block diagram showing the breaking and crushing procedure of the Campaign 9 blocks.

Statistical analysis was used to identify parameters which played a significant role in determining the final particle size distribution of the slag (as opposed to accurately predicting the absolute extent of fines generation and/or the residual coarse fraction). However, due to the limited number of blocks available, traditional statistical analysis could not be used. Statistical linear regression analyses were consequently applied to predict the *relative rating* of the blocks with regard to fines generation and residual coarse material**. From these ratings, parameters significant to particle size were identified, with their relative importance.

In order to test the validity of the relative importance of the statistically identified parameters, the actual relative rating of a block (in terms of fines generation and residual coarse mass) was compared with its rating as predicted by the regression coefficients. The difference between these two sets of ratings was quantified with a root-mean-square error (rms error) - a low rms error hence indicating a close correspondence between the actual and predicted ratings of the

** The residual coarse fraction is indicative of a higher or lower mill circulating mass, which in turn implies a higher or lower probability of generating more fines. This is termed “indirect” fines generation, in this study.

specific parameters and their relative importance. The coefficient of determination (r^2) of the regression analysis was considered to be of secondary importance (relative to the rms error).

Potential parameters which could influence fines generation and the residual coarse mass were identified based on two proposed hypotheses: (i) the final particle size distribution is a function of the block solidification structures, and (ii) the particle size distribution is a result of oxidation effects.

Should solidification structures play a role in slag breakage, evidence of intergranular breakage is expected. This could result in liberation of the silicate phases typically found between M_3O_5 grains. The parameter (SiO_2+$Al_2O_{3\ glass}$+CaO)†† was therefore included in the analysis.

Should oxidation effects play a role, the block cooling method, specific area of the block, and block chemistry (composition) should be considered:

- Whereas in the previous section block yield was used to quantify the fines generated *during cooling* (i.e. the extent of decrepitation), block yield was used in this context to quantify the effect of the cooling method on the fines generation during *crushing and milling*.

- The specific surface area of the block was calculated by approximating the block surface as the sum of a spherical cap and a truncated cone, and dividing this surface area by the block volume. Due to the mass loss of the blocks during cooling, the specific surface areas of the blocks both before (as tapped) and after cooling were considered.

- Since FeO, TiO_2 and Ti_2O_3 are interrelated, the equivalent $\%Ti_2O_3$ (calculated as per equation (2)[26], which is for analyses in mass percentages), was selected to represent the composition of the block. The Ti_2O_3 (Ti^{3+}) content of the slag is determined through a wet chemistry technique (Appendix 5.1). The correlation between FeO and Ti_2O_3 as determined from XRF and wet chemistry analyses during Campaign 9 is shown in Figure 14. Since only XRF analyses were done on the 11 blocks used in this investigation, the correlation as shown in Figure 14 was used to calculate the corresponding $\%Ti_2O_3$ of the specific blocks.

$$\left(\%Ti_2O_3\right)_{eq} = \%Ti_2O_3 + \%V_2O_5\left(\frac{M_{Ti_2O_3}}{M_{V_2O_5}}\right) + \%Cr_2O_3\left(\frac{M_{Ti_2O_3}}{M_{Cr_2O_3}}\right) + \left(\%Al_2O_3 - \frac{\%SiO_2}{3}\right)\left(\frac{M_{Ti_2O_3}}{M_{Al_2O_3}}\right) \quad (2)$$

†† The (SiO_2+$Al_2O_{3(glass)}$+CaO) content of the slag combines to form the glassy and crystalline silicate phases in the solidified slag. Some of the Al_2O_3 reports to the M_3O_5 solid solution where it replaces the Ti^{3+} atoms, while the remainder reports to the silicate phases. An amount of Al_2O_3 equal to a third of the SiO_2 content is assumed to report to the glass phase.

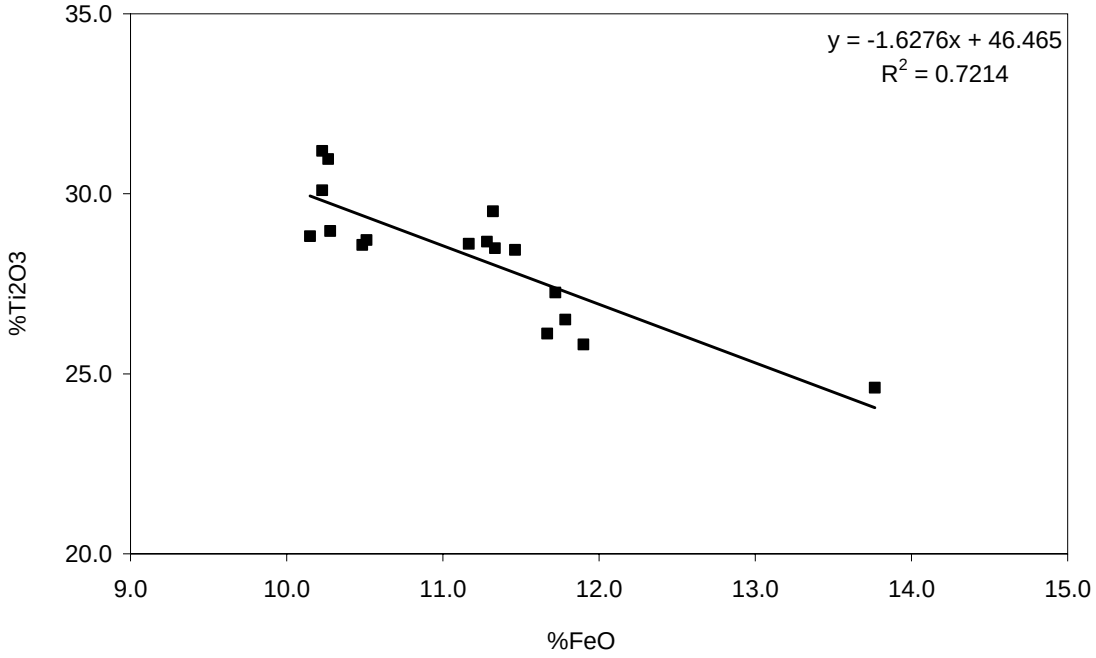

Figure 14 Correlation between FeO and Ti_2O_3 as analysed during the Campaign 9 trials.

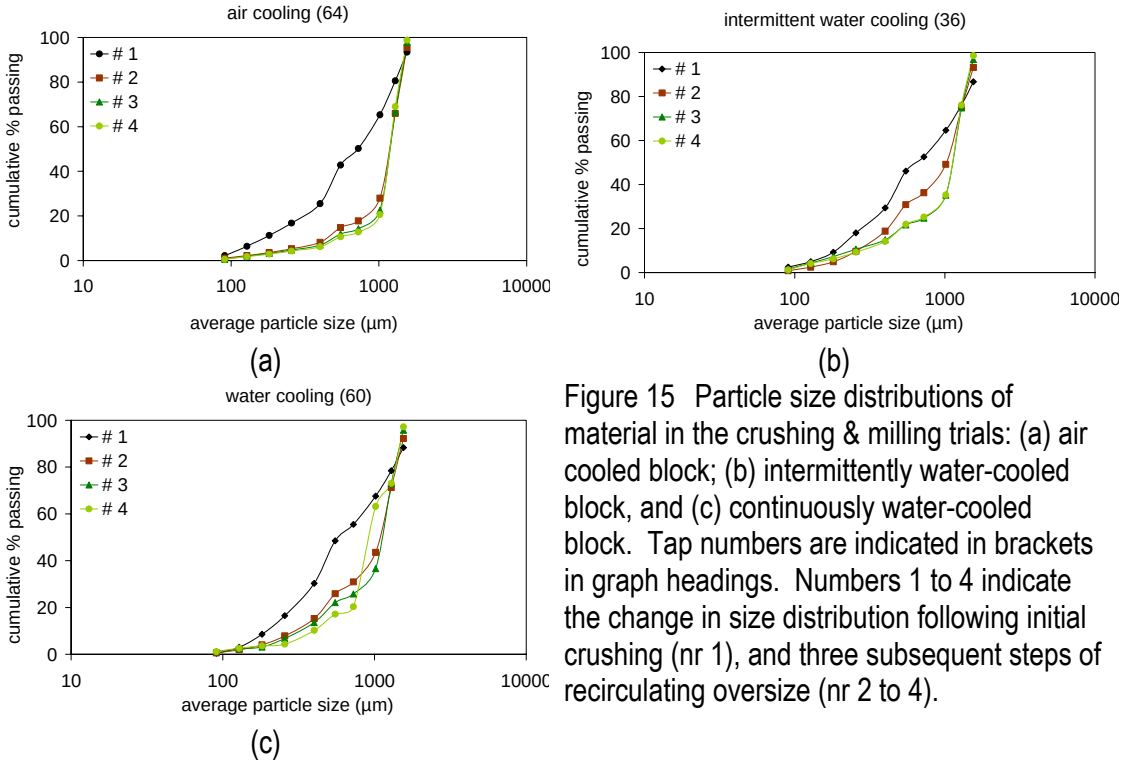

Figure 15 Particle size distributions of material in the crushing & milling trials: (a) air cooled block; (b) intermittently water-cooled block, and (c) continuously water-cooled block. Tap numbers are indicated in brackets in graph headings. Numbers 1 to 4 indicate the change in size distribution following initial crushing (nr 1), and three subsequent steps of recirculating oversize (nr 2 to 4).

2.3.2 Results

The particle size distributions of the product during the four milling steps of the air cooled block are shown in Figure 15. The -106 µm vs. +850 µm mass fractions have a linear log-log correlation (Figure 16). The majority of the fines are generated in the first step of milling. The absolute number of fines generated and residual coarse fraction shift slightly towards lower values from the second to the fourth milling steps.

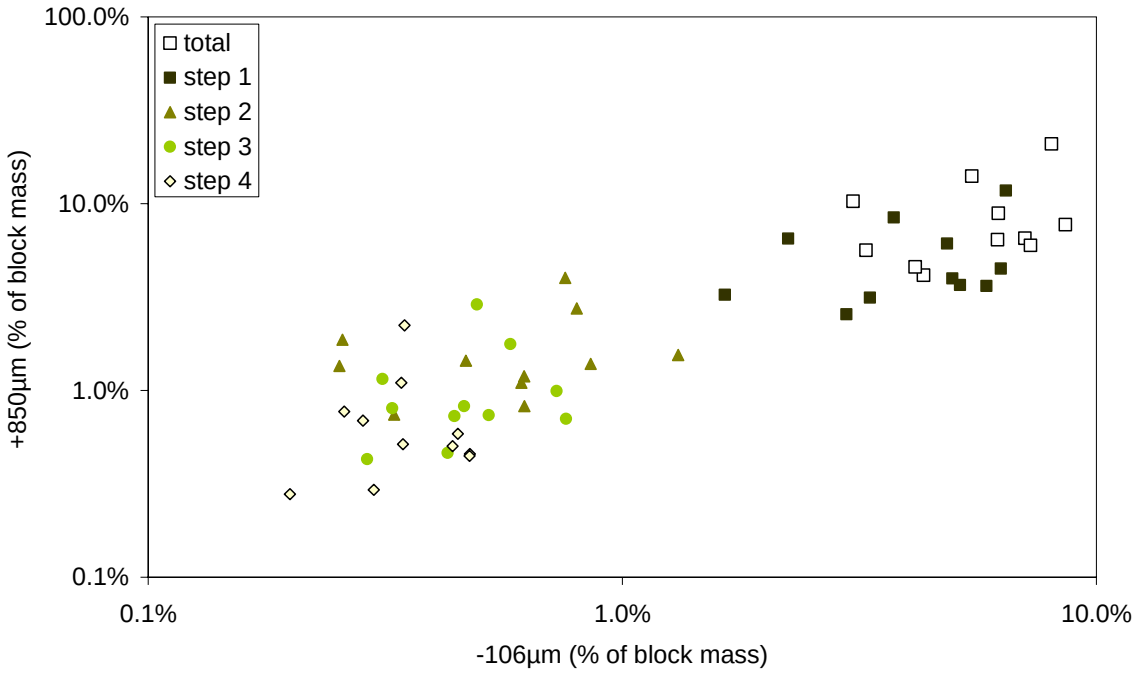

Figure 16 -106µm vs. +850µm mass percentages of the Campaign 9 crushed blocks.

2.3.2.1 **Fines generation (-106 µm size fraction)**

The cumulative fines generated for each block, arranged from worst to best (least), are shown in Figure 17. The intermittently water-cooled and air-cooled blocks cover the worst end of the graph, while the pot-cooled blocks and repeatedly submerged block yielded the smallest amount of fines.

Statistical linear regression analysis on the total amount of -106 µm material generated during milling and several parameters generated the correlation coefficients as shown in Table 3. (A complete list of all parameters which were tested for correlation is given in Appendix 5.2. These statistical results should be interpreted bearing in mind that only 11 blocks were used in the analysis.) Significant improvements of the correlation coefficients were observed in some instances when omitting one or two blocks from the regression analysis. This effect was interpreted as indicative of the presence of a dominant factor with regard to fines generation in the omitted block.

The correlation coefficient between the fines generated and the (SiO_2+$Al_2O_{3(glass)}$+CaO) content of the slag is 0.717. This number increases to 0.774 and 0.787 when excluding water-cooled block 49 and intermittent water-cooled block 36. Excluding both these blocks increased the value of the correlation coefficient to 0.836. The positive sign of the correlation coefficient indicates a direct linear correlation between the (SiO_2+$Al_2O_{3(glass)}$+CaO) content and fines generated. The fines generated per block is shown in Figure 18 in order of increasing (SiO_2+$Al_2O_{3(glass)}$+CaO). The average fines generated appears to be lower for blocks with (SiO_2+$Al_2O_{3(glass)}$+CaO) contents below 1.93% (the four blocks on the left in Figure 18) when compared with the average fines generated from the remainder of the blocks.

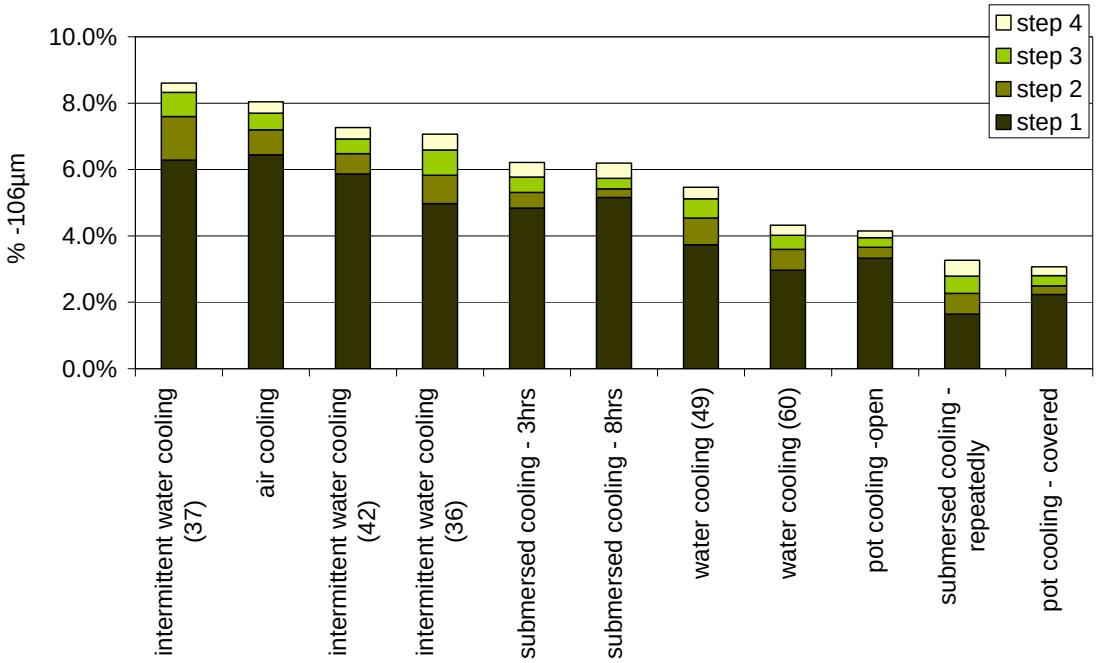

Figure 17 Mass percentage fines generated (-106 µm fraction) per milling step 1 to 4, shown per cooling method (tap numbers are shown in brackets), arranged from worst to least fines generation.

Table 3 Correlation coefficients of parameters affecting the fines generation during crushing & milling.

Variable	Correlation coefficient (including all 11 blocks)	Best correlation coefficient	Exclusions
%SiO_2+$Al_2O_{3(glass)}$+ CaO	0.717	0.774	Water cooled (49)
		0.787	Intermittent water cooled (36)
		0.836	water cooled (49) & intermittent water cooled (36)
Tapping rate‡‡	-0.353	-0.733	Covered pot cooled (44)
		-0.728	Intermittent water cooled (37)
Block yield	-0.280	-0.492	Intermittent water cooled (37)
Equivalent %Ti_2O_3	0.109	0.367	Air cooled block (64)
Specific surface area – cooled block	0.278	0.624	Intermittent water cooled (37)
		0.481	Covered pot cooled (44)
Specific surface area – as tapped block	0.051	0.256	Intermittent water cooled (37)

‡‡ The tapping rate was calculated by dividing the as tapped block mass (in kg) by the total tapping time (in minutes). The total tapping time was calculated as the time difference between opening (observing the first slag flow) and closing of the taphole).

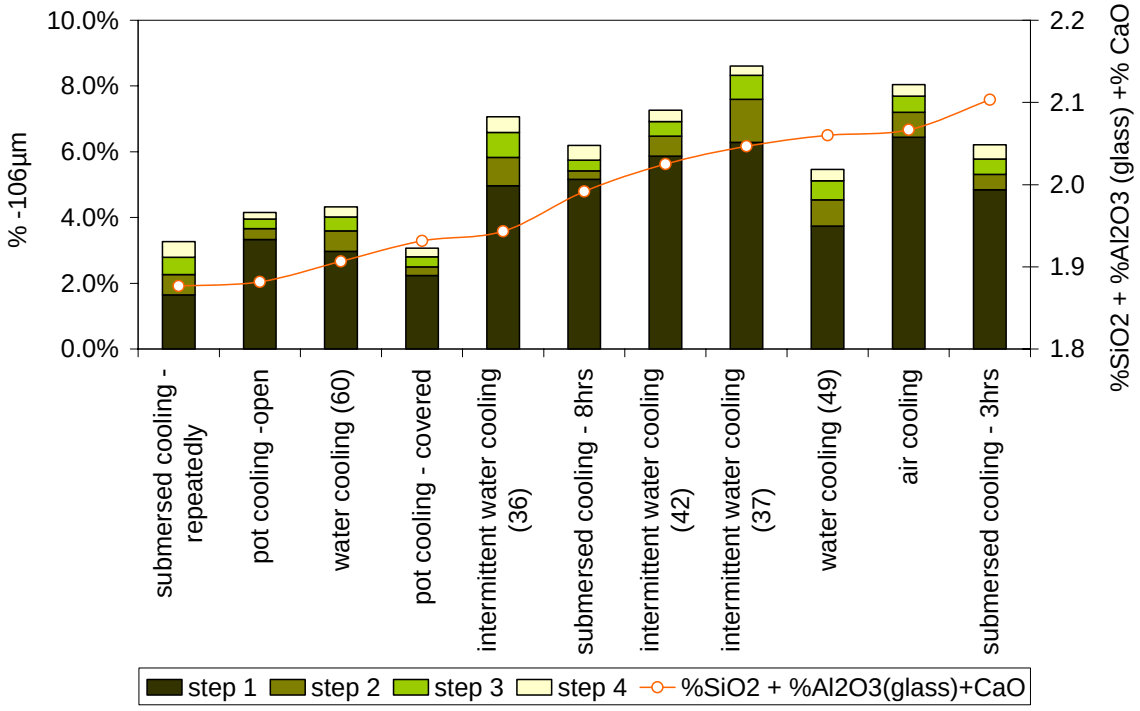

Figure 18 Mass percentage fines generated (-106 µm) ordered with increasing ($\%SiO_2+Al_2O_{3(glass)}+CaO$).

Exclusion of the covered pot 44 and intermittently water-cooled pot 37 increases the correlation coefficient between the fines generated and the tapping rate from -0.353 to -0.733 and -0.728 respectively. The negative sign of the coefficient indicates an indirect correlation – higher tapping rates correlate with reduced fines generation. The fines generation ordered with increasing tapping rate is shown in Figure 19.

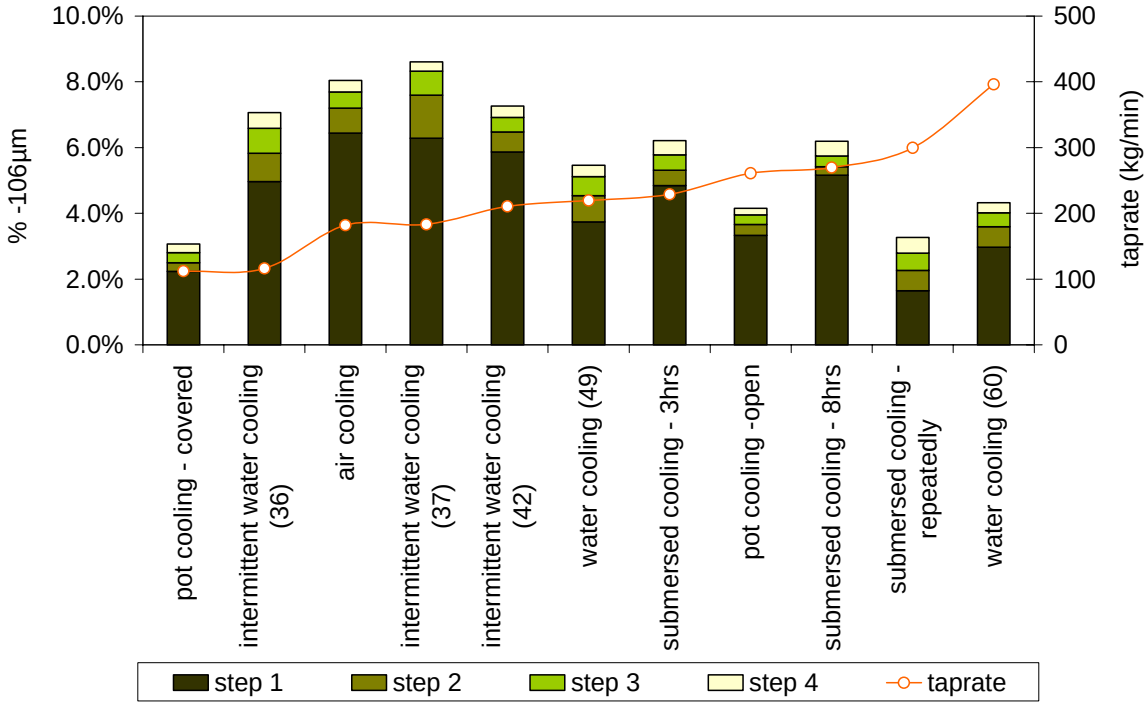

Figure 19 Mass percentage -106µm generated shown against increasing tapping rate.

Correlation coefficients between the fines generated and the block yield and $\%Ti_2O_3$ respectively were low (Table 3). Of potential value, however, is the sign of these correlation coefficients: an indirect correlation between the fines generated and the block yield indicates that good cooling method practices have a positive influence on reducing fines generation. The maximum coefficient (obtained when excluding air cooled block 64) between $\%Ti_2O_3$ and fines generation is positive. However, its sign changes to negative when either intermittently water-cooled block 37 or the covered pot block is excluded from the analysis, so the effect is not clear.

The correlation coefficients between the fines generated and the two different specific block surface areas are also low – in particular that for the as-tapped block (Table 3). However, the coefficient increases significantly – from 0.278 to 0.624 - for the cooled block when omitting the intermittently water-cooled block 37. Of possible significance when considering the difference in correlation coefficients of the two specific surface areas is the time lapse of approximately four months between the blocks being tapped and their actual breaking, crushing and subsequent particle size determination.

Regression analysis including the glass phase content (SiO_2+$Al_2O_{3(glass)}$+CaO) and tapping rate only resulted in an rms error between the actual and predicted relative ratings of the blocks of 2.5 and a coefficient of determination (r^2) of 0.53. Including the $\%Ti_2O_3$, block yield and specific surface area after cooling into the regression analysis reduced the rms error to 1.4, with a coefficient of determination (r^2) at 77.2% indicating that the fines generation of between 8 and 9 of the 11 blocks could be explained by the five block attributes (SiO_2+$Al_2O_{3(glass)}$+CaO), tapping rate, block yield, equivalent $\%Ti_2O_3$ and specific surface area after cooling – in this order of importance. A comparison of the worst to best relative position of the actual and regression results is shown in Table 4.

Table 4 Comparison of the experimental worst to best ranking and that predicted by the regression model when including the (SiO_2+$Al_2O_{3(glass)}$+CaO), tapping rate, block yield, specific surface area after cooling and equivalent $\%Ti_2O_3$.

Cooling method and block number		Experimental rating	Regression model rating	Deviation in relative rating
air cooling	64	10	9	-1
water & air cooling	36	8	8	0
water & air cooling	37	11	11	0
water & air cooling	42	9	7	-2
water cooling	49	5	5	0
water cooling	60	4	4	0
submersion cooling - 3hrs	47	7	10	3
submersion cooling - 8hrs	43	6	6	0
submersion cooling – repeatedly	65	2	2	0
pot cooling – open	62	3	1	-2
pot cooling - covered	44	1	3	2
Root-mean-square (rms) error				1.4

2.3.2.2 **Residual coarse material (+850 µm size fraction)**

The residual coarse mass (after four milling passes) is shown in Figure 20, arranged in order from worst (highest) to lowest. A larger amount of residual coarse material is viewed as undesirable, since such material would circulate to be recrushed, in the industrial plant. Such

circulation is expected to increase the proportion of fine material; this is termed "indirect fines generation" in this work, in contrast with "direct fines generation", which refers to the fine material which forms during initial crushing. The order of blocks in Figure 20 differs substantially from that in Figure 17 (which is the corresponding graph for the fines generated). It therefore appears that the parameters influencing fines generation differ from those influencing the residual coarse mass, and/or the relative importance of the parameters differs for the two size fractions.

The correlation coefficients between the residual coarse mass and six potential parameters are shown in Table 5 (a complete list of all parameters considered is shown in Appendix 5.2).

The specific surface area of the cooled block has a significant correlation coefficient of 0.846 which increases to 0.915 when air-cooled block 64 is omitted. The positive sign of the coefficient indicates a tendency for more residual coarse mass with increasing specific surface area. The residual coarse fractions arranged in order of increasing specific surface area of the cooled blocks are shown in Figure 21. The increase in the correlation coefficient between the specific surface area of the *tapped* block and the residual coarse mass with the exclusion of the air-cooled block 64, is more likely due to the interdependency between the two different surface areas.

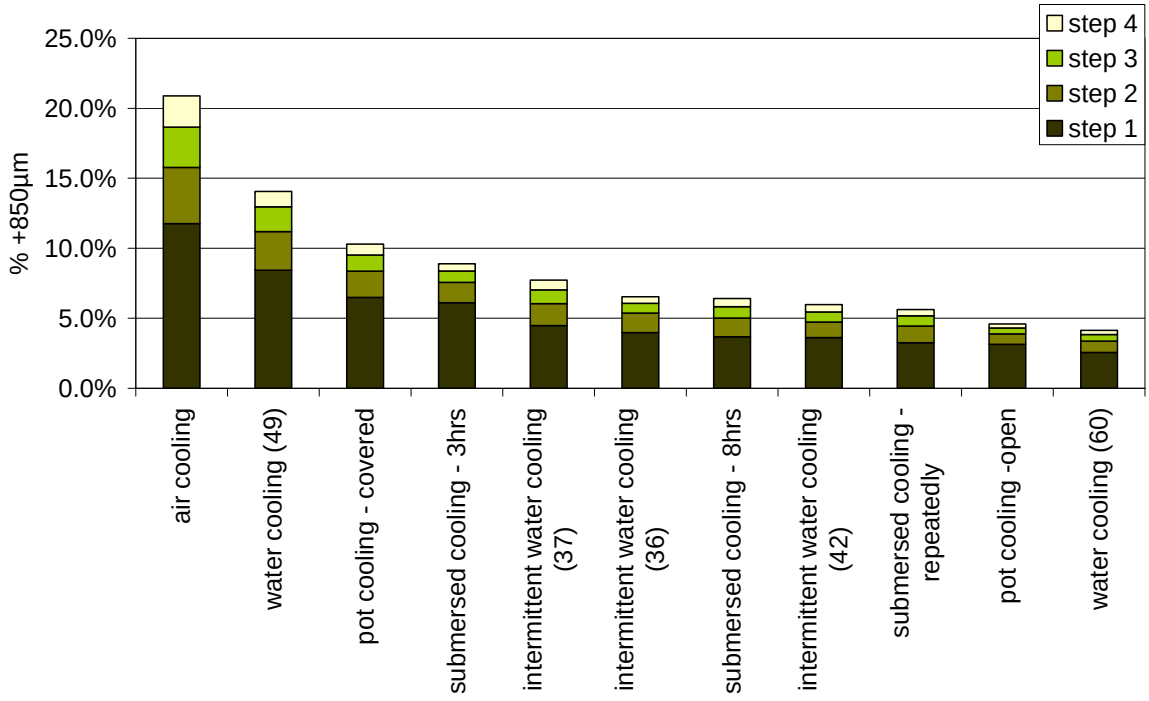

Figure 20 Mass percentage residual coarse fraction (+850µm) ordered from worst to best.

Table 5 Correlation coefficients of independent variables affecting the residual coarse fractions during crushing. The best correlation coefficients were obtained by excluding the blocks named in the right hand column.

Variable	Correlation coefficient (all 11 blocks analysed)	Best correlation coefficient	Exclusions
Specific surface area – cooled block	0.846	0.915	Air cooled (64)
Specific surface area – as tapped block	0.242	0.901	Air cooled (64)
Block yield	-0.807	-0.924	Water cooled (49)
		-0.866	Open pot cooled (62)
$\%SiO_2+Al_2O_{3(glass)}+CaO$	0.591	0.666	Water & air cooled (37)
		0.634	Covered pot cooled (44)
Tapping rate	-0.415	-0.539	Water & air cooled (36)
Equivalent $\%Ti_2O_3$	-0.263	-0.488	Water cooled (49)

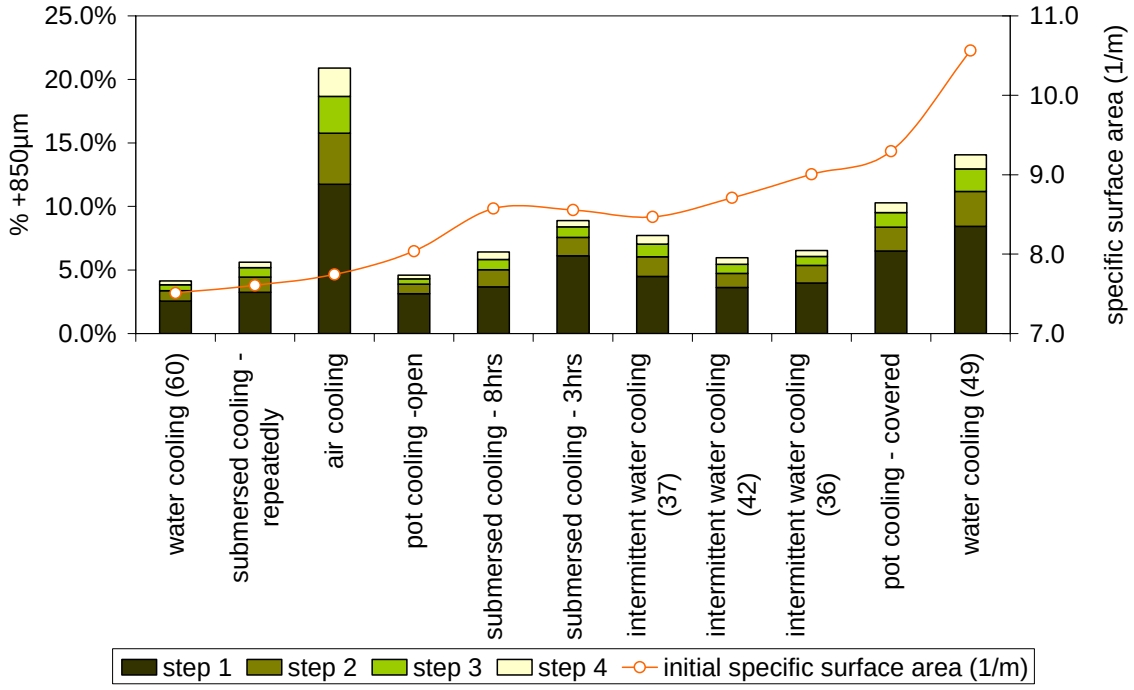

Figure 21 Residual coarse fractions arranged in order of increasing specific surface area of the blocks – after cooling.

The cooling method as quantified by the block yield has a correlation coefficient of -0.807 with the residual coarse fraction. Omitting water-cooled block 49 and the open-pot-cooled block 62, the coefficient increases to -0.924 and -0.866 respectively. The negative sign of the coefficient indicates and indirect correlation - less residual coarse mass is associated with higher block yields. The residual coarse fraction from each block arranged in order of increasing block yield is shown in Figure 22.

The correlation coefficients between the residual coarse mass and the three parameters: glass phase, tapping rate and $\%Ti_2O_3$, showed lower and insignificant values – even when omitting

seemingly outlying blocks. The residual coarse fractions arranged in order of increasing parameter are shown in Figure 23, Figure 24 & Figure 25.

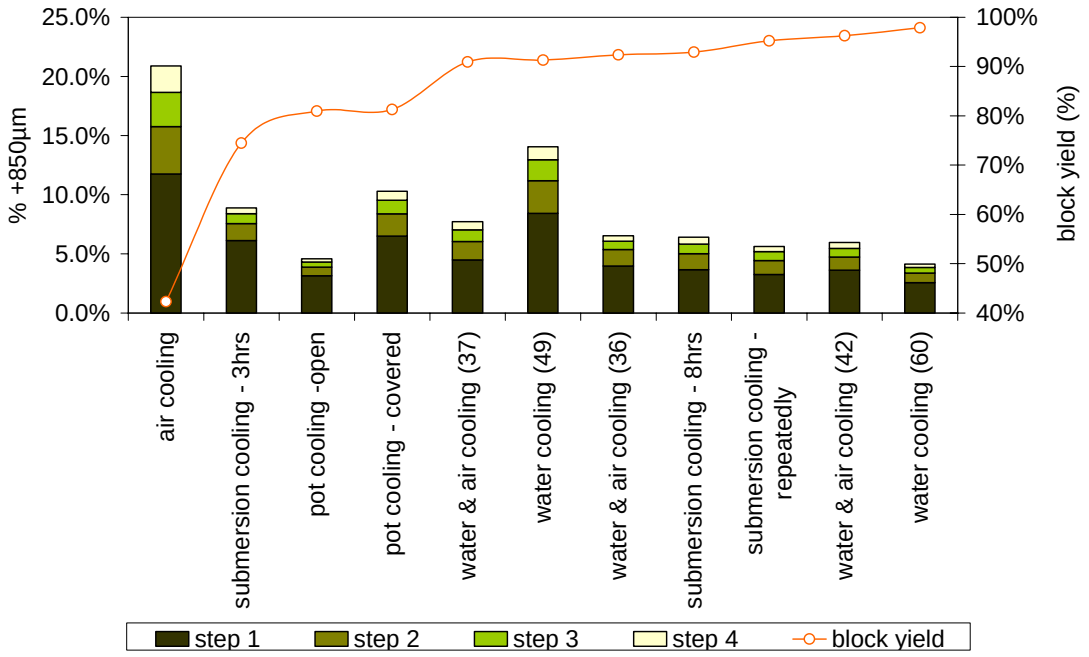

Figure 22 Residual +850 µm with increasing block mass yield.

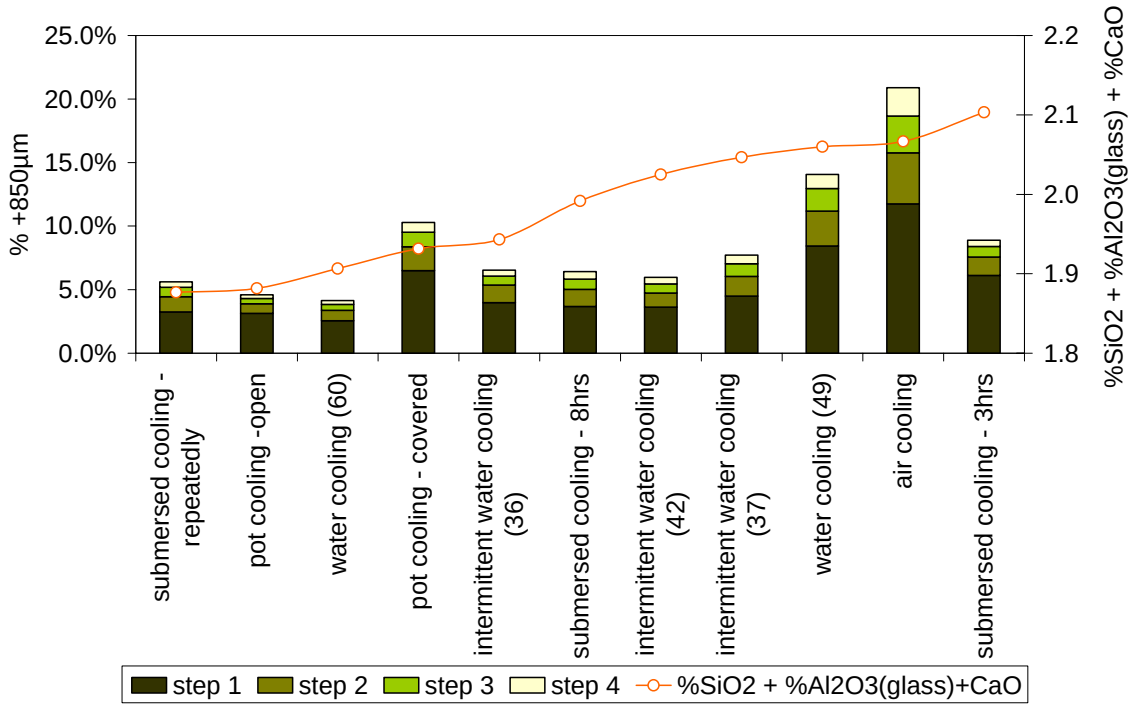

Figure 23 Residual coarse fraction arranged in order of increasing (SiO_2+$Al_2O_{3(glass)}$+CaO).

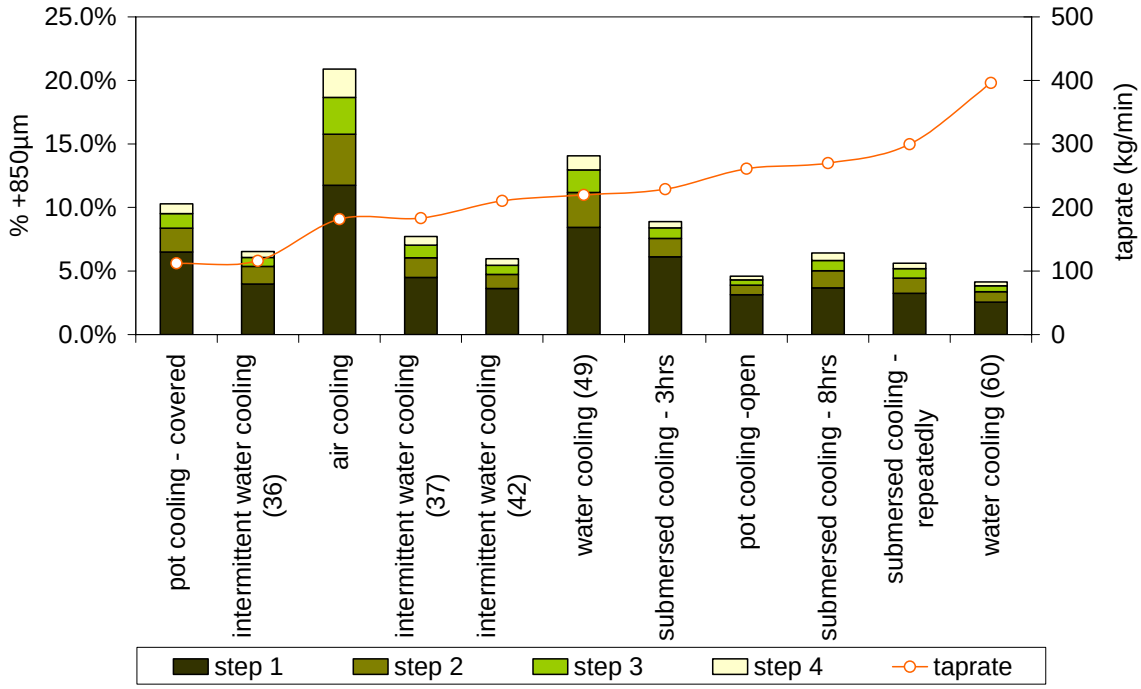

Figure 24 Residual coarse fraction arranged in order of increasing tapping rate.

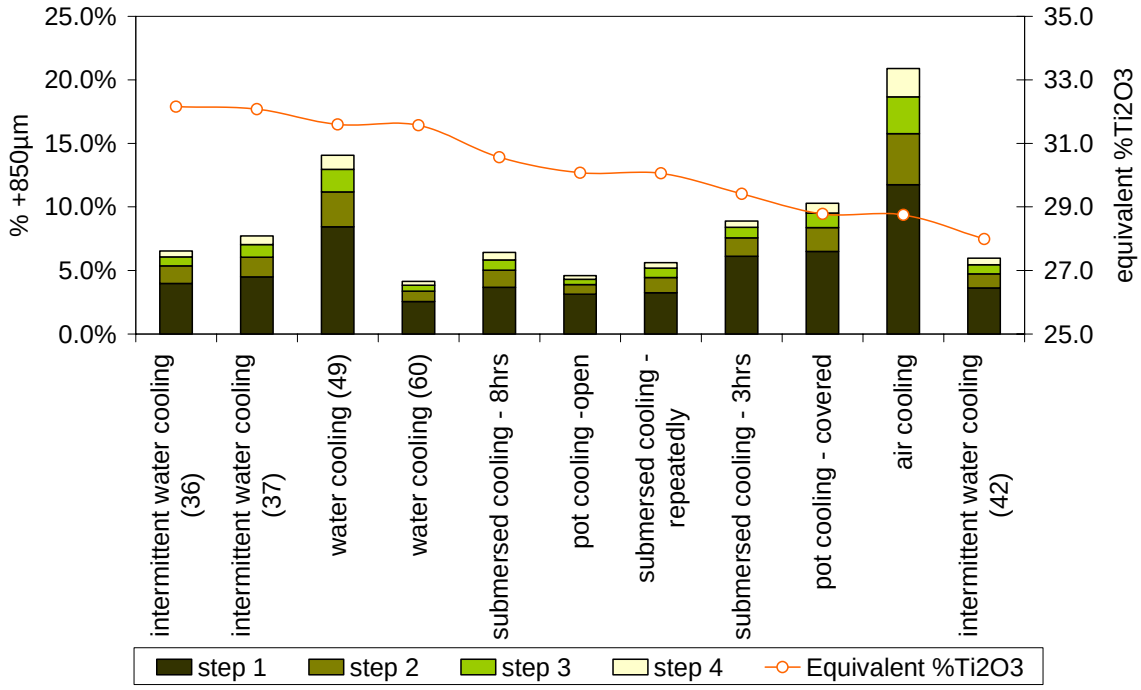

Figure 25 Residual coarse fraction arranged in order of increasing equivalent Ti_2O_3.

Similar to the parameter testing with fines generation, the actual relative order of the blocks with regard to residual coarse mass was compared with that predicted by the regression analysis. Including only the specific surface area after cooling and the block yield in the regression analysis resulted in an rms error of 1.7. (The coefficient of determination of the regression analysis r^2, was 0.860; hence explaining the residual coarse mass for 86% of the blocks – between 9 to 10 of the 11 blocks.) Although the best improvement in the coefficient of

determination (reaching 0.885) results from including all five parameters block yield, specific surface area after cooling, tapping rate, (SiO_2+$Al_2O_{3(glass)}$+CaO) and equivalent %Ti_2O_3, the rms error for this combination is 2.0. The lowest rms error results from the combination block yield, specific surface area after cooling and (SiO_2+$Al_2O_{3(glass)}$+CaO) – 1.5 with a coefficient of determination of 0.863. The comparison between the actual worst to best order and the predicted worst to best order from the regression analysis which included the latter three parameters is shown in Table 6.

Table 6 Comparison between the actual worst to best order and the predicted order (including the block yield, specific surface area after cooling and glass phase variables).

Cooling method and block number		Experimental ranking	Regression model ranking	Deviance in relative rating
air cooling	64	11	11	0
water & air cooling	36	6	7	1
water & air cooling	37	7	5	-2
water & air cooling	42	4	3	-1
water cooling	49	10	10	0
water cooling	60	1	1	0
submersion cooling - 3hrs	47	8	9	1
submersion cooling - 8hrs	43	5	4	-1
submersion cooling – repeatedly	65	3	2	-1
pot cooling - open	62	2	6	4
pot cooling - covered	44	9	8	-1
Root-mean-square (rms) error				1.5

2.3.3 Conclusions

Dominant parameters influencing the *fines generation* (-106 µm) in order of importance, starting with the most important, are therefore concluded to be:

- The amount of glass phase (SiO_2+$Al_2O_{3(glass)}$+CaO);
- Tapping rate;
- Cooling method as quantified by the block yield;
- Specific surface area of the block after cooling, and
- Block composition as represented by the %Ti_2O_3.

The amount of glass phase present and tapping rate explain the fines generation of approximately half of the blocks. Including the other three parameters - specific surface area after cooling, block yield and equivalent %Ti_2O_3 increases the accuracy of the linear regression analysis to 79% (accurately predicting the relative rating of between 8 to 9 of the 11 blocks). The root-mean-square (rms) error between the actual rating of worst to best performance compared to similar predicted order is 1.5.

The dominant parameters influencing the *residual coarse mass* (+850 µm after four milling passes) in order of importance; starting with the most important, are concluded to be:

- Specific surface area of the block after cooling;
- Cooling method as quantified by the block yield;
- The amount of glass phase (SiO_2+$Al_2O_{3(glass)}$+CaO);

- Tapping rate, and
- Block composition as represented by the $\%Ti_2O_3$.

The specific surface area after cooling, and block yield, explain the residual coarse fractions of 86% (between 9 to 10 out of 11) of the blocks. The inclusion of (SiO_2+$Al_2O_{3(glass)}$+CaO), tapping rate and equivalent $\%Ti_2O_3$ improves the root-mean-square error of the actual vs. predicted orders and/or the coefficient of determination (r^2) slightly - e.g. improving the rms error from 1.7 to 1.5 when including the glass phase, or increasing the r^2 from 0.86 to 0.89 when including all five parameters.

2.3.3.1 **Slag composition and mineralogy**

Excluding the air-cooled block 64 from the analysis results in a negative correlation coefficient between the $\%Ti_2O_3$ and residual coarse mass. However, inclusion of air-cooled block 64 in the analysis yields a positive coefficient. Similar dual behaviour of the $\%Ti_2O_3$ is seen with fines generation. The dual behaviour of slag composition – as represented by the equivalent $\%Ti_2O_3$ – suggests that the composition is of secondary importance with regard to direct and indirect fines generation.

As in the case of fines generation, the sign of the coefficient between the glass phase and the residual coarse mass is positive. A higher glass phase therefore results in more fines generation, both directly and indirectly (the latter via a higher circulating load). The importance of the glass phase indicates that the generation of fines (directly and indirectly) occurs through a mechanism which is associated with the solidification structure.

2.3.3.2 **Tapping rate**

The sign of the correlation coefficients between fines generation and tapping rate indicates a tendency for decreased fines generation due to higher tapping rates; while the coefficient between residual coarse mass and tapping rate indicates potential for an increase in fines generation due to a higher circulating load. The effect of tapping rate is presumed to operate through one or both of the following mechanisms:

- Lower tapping rates are characterised by increased oxygen lancing by the tapping personnel (in an attempt to improve the flow). This action in itself creates an oxidising atmosphere.

- Lower tapping rates result in spraying tap streams – creating an increased specific slag surface area which is exposed to air while the slag flows from the launder into the pot. Due to the high slag temperatures at this stage (1600 °C – 1720 °C), oxidation is highly likely.

Should either or both of the two mechanisms occur – which is regarded as highly likely due to the high temperatures and excess oxygen present– the link between tapping rate, and fines generation and residual coarse fraction, is based on an oxidation mechanism. Oxidised slag will contain more rutile in the solidified microstructure (as discussed in section 1); it appears that this favours fines formation.

2.3.3.3 **Block surface area**

The oxidation hypothesis is supported by the inclusion of the specific surface area after cooling, and the cooling method, amongst the important parameters for both fines generation and residual coarse fractions: further oxidation is expected to occur during the cooling period while the surface is still at relatively high temperatures. The significant difference between the correlation coefficients of the specific surfaces of the as “tapped surface” and the “after cooling surface”, combined with the four-month time lapse between the tapping and breaking activities suggests the possibility that oxidation at low temperatures (< 200 °C) may also affect fines generation. This was studied further, and the results are reported in section 3.7.

The influence of the three parameters, slag mineralogy, tapping rate and block surface area, is discussed further in Part 2 of this document.